J|A|C|S
ARTICLES
Published on Web 01/13/2004

Mapping the Electronic Structure of the Blue Copper Site in Plastocyanin by NMR Relaxation

D. Flemming Hansen and Jens J. Led*

Contribution from the Department of Chemistry, University of Copenhagen, Universitetsparken 5, DK-2100 Copenhagen Ø, Denmark

Received August 15, 2003; E-mail: led@kiku.dk

Abstract: The biological function of metalloproteins stems from the electronic and geometric structures of their active sites. Thus, in blue copper proteins such as plastocyanins, an unusual electronic structure of the metal site is believed to contribute to the rapid, long-range electron-transfer reactivity that characterizes these proteins. To clarify this structure−function relationship, numerous quantum chemical calculations of the electronic structure of the blue copper proteins have been made. However, the obtained structures depend strongly on the applied model. Experimental approaches based on ENDOR spectroscopy and X-ray absorption have also been used to elucidate the electronic structure of the blue copper site. Still, the determination of the electronic structure relies on a calibration with quantum chemical calculations, performed on small model complexes. Here we present an approach that allows a direct experimental mapping of the electron spin delocalization in paramagnetic metalloproteins using oxidized plastocyanin from *Anabaena variabilis* as an example. The approach utilizes the longitudinal paramagnetic relaxation of protons close to the metal site and relies on the dependence of these relaxations on the spatial distribution of the unpaired electron of the metal ion. Surprisingly it is found that the unpaired electron of the copper ion in plastocyanin is less delocalized than predicted by most of the quantum chemical calculations.

Introduction

Metal ions play a key role in the function of metalloproteins, such as the electron-transporting blue copper proteins, plastocyanins, and the azurins.[1,2] Unlike small-molecule copper complexes, these proteins have an unusual geometry of the coordination sphere (Figure 1),[3−8] a high redox potential,[9] and a large and asymmetric delocalization of the unpaired electron spin density onto the ligands,[1,2,10−15] including a strong covalency of a copper−sulfur bond. The rapid and long-range electron transfer reactivity that characterizes the blue copper proteins is believed to rely on this unusual electronic structure of the metal site.[2]

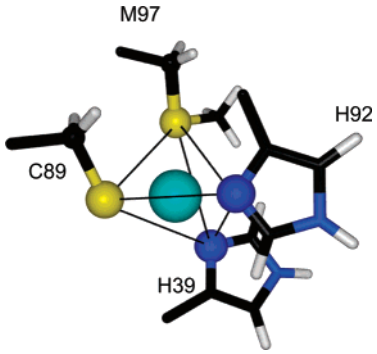

Figure 1. Coordination sphere of the catalytic site in *A.v.* PCu[16] (PDB: 1FA4). The site has a distorted tetrahedral geometry with the copper ion strongly bound to the S^{γ} atom of the cysteine C89 and to the N^{δ} atoms of the two histidines H39 and H92 but weakly bound to the axial S^{δ} atom of M97.

Therefore, during the last few decades, the blue copper proteins have become a reference point for quantum chemical calculations aimed at the elucidation of the electronic structure−function relationship of metalloproteins.[1,2,10−12] Thus, pioneering quantum chemical studies of the electronic structure of the metal site of plastocyanin and other blue copper proteins were made in the 1980s by Solomon and co-workers,[1,2] using the semiem-

* To whom correspondence should be addressed.

(1) Penfield, K. W.; Gewirth, A. A.; Solomon, E. I. *J. Am. Chem. Soc.* **1985**, *107*, 4519−4529.
(2) Solomon, E. I.; Lowery, M. D. *Science* **1993**, *259*, 1575−1581.
(3) Colman, P. M.; Freeman, H. C.; Guss, J. M.; Murata, M.; Norris, V. A.; Ramshaw, J. A. M.; Venkatappa, M. P. *Nature* **1978**, *272*, 319−324.
(4) Guss, J. M.; Freeman, H. C. *J. Mol. Biol.* **1983**, *169*, 521−563.
(5) Bond, C. S.; Bendall, D. S.; Freeman, H. C.; Guss, J. M.; Howe, C.; Wagner, M. J.; Wilce, M. C. *Acta Crystallogr. Biol. Crystallogr.* **1999**, *D55*, 414−421.
(6) Inoue, T.; Sugawara, H.; Hamanaka, S.; Tsukui, H.; Suzuki, E.; Kohzuma, T.; Kai, Y. *Biochemistry* **1999**, *38*, 6063−6069.
(7) Inoue, T.; Gotowda, M.; Sugawara, H.; Kohzuma, T.; Yoshizaki, F.; Sugimura, Y.; Kai, Y. *Biochemistry* **1999**, *38*, 13853−13861.
(8) Shibata, N.; Inoue, T.; Nagano, C.; Nishio, N.; Kohzuma, T.; Onodera, K.; Yoshizaki, F.; Sugimura, Y.; Kai, Y. *J. Biol. Chem.* **1999**, *7*, 4225−4230.
(9) Sanderson, D. G.; Anderson, L. B.; Gross, E. L. *Biochim. Biophys. Acta* **1986**, *852*, 269−278.
(10) Pierloot, K.; De Kerpel, J. O. A.; Ryde, U.; Roos, B. O. *J. Am. Chem. Soc.* **1997**, *119*, 218−226.
(11) Pierloot, K.; De Kerpel, J. O. A.; Ryde, U.; Olsson, M. H. M.; Roos, B. O. *J. Am. Chem. Soc.* **1998**, *120*, 13156−13166.
(12) vanGastel, M.; Coremans, J. W. A.; Sommerdijk, H.; Hemert, M. C.; Groenen, E. J. J. *J. Am. Chem. Soc.* **2002**, *124*, 2035−2041.
(13) Werst, M. M.; Davoust, C. E.; Hoffman, B. M. *J. Am. Chem. Soc.* **1991**, *113*, 1533−1538.
(14) Shadle, S. E.; Penner-Hahn, J. E.; Schugar, H. J.; Hedman, B.; Hodgson, K. O.; Solomon, E. I. *J. Am. Chem. Soc.* **1993**, *115*, 767−776.
(15) George, S. J.; Lowery, M. D.; Solomon, E. I.; Cramer, S. P. *J. Am. Chem. Soc.* **1993**, *115*, 2968−2969.

pirical self-consistent field Xα scattered-wave (SCF-Xα-SW) method. These studies indicated a substantial covalency of the metal−ligand bonds, that is, a 40% copper and a 36% sulfur character of the singly occupied molecular orbital (SOMO) in the ground state of the oxidized protein. Recent quantum chemical calculations, using more stringent ab initio calculations[10−12] and small model complexes, also pointed toward a delocalization of the electron spin onto the ligands. However, the calculated ligand character of the SOMO varied from 20 to 60% depending on the applied quantum chemical approach and the applied model complex. Thus, it was found that variations of the structure of the model complex within the uncertainties of the X-ray structure strongly influence the calculated SOMO.[10]

Approaches that include experimental solid-state measurements based on electron−nuclear double-resonance coupling (ENDOR)[13] and X-ray absorption[14,15] have also been used to clarify the electronic structure of the blue copper site. Yet, the spin delocalizations thus obtained rely on a calibration with the results of quantum chemical calculations of small model complexes. More specifically, the isotropic hyperfine coupling constant of the ligand N^{δ} atoms was determined in Q-band ^{14}N ENDOR experiments. Subsequently, a calibration using quantum calculations on the small copper complex, $[Cu(imidazole)_4]^{2+}$, resulted in a 5% delocalization of the unpaired electron on each of the N^{δ} ligand atoms.[13] The X-ray absorption experiments were previously used to determine the ligand character of the SOMO.[14,15] In these studies, the delocalization of the unpaired electron onto the cysteine sulfur ligand was estimated, however, still on the basis of a calibration using quantum chemical calculations of small copper complexes.

An independent experimental determination of the electronic structure is, therefore, of interest in order to obtain better insight into the long-range and rapid electron-transfer reactivity of the blue copper proteins. Here we present a method that allows such a determination. The method is based on a direct experimental mapping of the electron spin delocalization. It exploits the rates of the electron-induced longitudinal relaxation (the longitudinal paramagnetic relaxation enhancement) of the protons in the vicinity of the metal ion, and it relies on a precise experimental determination of these rates.

Theory

The paramagnetic relaxation of the protons close to the metal site is strongly affected by the delocalization of the unpaired electron spin onto the ligand atoms of the metal site. This is unlike the paramagnetic relaxation of the more distant protons (more than 11 Å from the metal ion), which can be described by the point dipole approximation[17,18] corresponding to an effective location of the electron spin on the metal ion. Therefore, if the paramagnetic relaxation rates can be obtained for a number of isotropically distributed protons close to the metal ion, a mapping of the electron delocalization can, in principle, be derived from these rates. However, until recently, an experimental determination of very fast nuclear relaxation rates was difficult. The newly developed SERF experiment[19] alleviates this problem, making it possible to measure the fast relaxation rates of nuclei close to a paramagnetic metal center.

The longitudinal paramagnetic relaxation enhancement, R_{1p}, of the nuclei in a paramagnetic metal complex is caused by the time-dependent modulation of the nuclear-electron spin interactions. These interactions are the dipolar interaction (through space) and the Fermi contact interaction (through bonds). Because of the relatively long electron relaxation time in blue copper proteins,[20] the longitudinal relaxation enhancement of the protons are to a good approximation affected only by the dipolar interaction, which is given by[17,18]

$$R_{1p} = \frac{2}{5}\left(\frac{\mu_0}{4\pi}\right)^2 S(S+1) g_{eff}^2 \mu_B^2 \gamma_I^2 \Delta^2 \frac{\tau_{c,1}}{1+\omega_I^2 \tau_{c,1}^2} \qquad (1)$$

Here, μ_0 is the magnetic permeability of free space, S is the spin quantum number of the unpaired electron(s), g_{eff} is the effective electron g-factor, μ_B is the Bohr magnetron, γ_I is the nuclear gyromagnetic ratio, and ω_I is the Larmor frequency of the nuclei. Furthermore, $\tau_{c,1}$ is the correlation time for the modulation of the nuclear-electron dipolar interaction. It is given by $\tau_{c,1}^{-1} = \tau_R^{-1} + R_{1e}$, where R_{1e} is the longitudinal relaxation rate of the unpaired electron, and τ_R is the rotational correlation time of the protein. Finally, Δ^2 is a geometric factor that contains the information about the location of the electron relative to the nucleus. If the point dipole approximation applies, as assumed in Solomon's original formalism,[17] Δ^2 is equal to r^{-6}, where r is the geometric distance between the nucleus and the unpaired electron. However, if the unpaired electron is delocalized onto the ligand nuclei, Δ^2 depends on the wave function describing the unpaired electron and its spatial distribution. If the wave function of the unpaired electron is known, the geometric factor is given by[18]

$$\Delta^2 = \frac{4\pi}{5}\sum_{\nu=-2}^{2}\left|\int_V d\mathbf{r}\ \Psi(\mathbf{r})^* F_2^{\nu}(\mathbf{r}')\Psi(\mathbf{r})\right|^2 \qquad (2)$$

where $\Psi(\mathbf{r})$ is the wave function of the unpaired electron(s), $F_2^{\nu}(\mathbf{r}') = Y_2^{\nu}(\theta',\phi')r'^{-3}$ represents the spatial components of the electron−nucleus dipolar operator centered at the nucleus, and $Y_2^{\nu}(\theta,\phi)$, $\nu = -2, ..., 2$, is the surface spherical harmonics. Furthermore, an asterix denotes complex conjugation. Thus, the electron delocalization can be taken into account explicitly in eq 1, if the wave function of the unpaired electron is known.[1,2] The total wave function Ψ can be written as a linear combination of atomic orbitals:

$$\Psi(\mathbf{r}) = N^{-1/2}\sum_{i}^{I}\sqrt{\rho_i}\psi_i(\mathbf{r}) \qquad (3)$$

where N is a normalization constant and ρ_i is the spin density in the individual orbitals. The spin densities are assumed to be positive and real. Thus, the geometric factor Δ^2 in eqs 1 and 2 can be written as

$$\Delta^2 = \frac{4\pi}{5N^2}\sum_{\nu=-2}^{2}\left|\sum_{i,j}\sqrt{\rho_i\rho_j}\int_V d\mathbf{r}\ \psi_i(\mathbf{r})^* F_2^{\nu}(\mathbf{r}')\psi_j(\mathbf{r})\right|^2 \qquad (4)$$

(16) Ma, L.; Jørgensen, A.-M. M.; Sørensen, G. O.; Ulstrup, J.; Led, J. J. *J. Am. Chem. Soc.* **2000**, *122*, 9473−9485.
(17) Solomon, I. A. *Phys. Rev.* **1955**, *99*, 559−565.
(18) Gottlieb, H. P. W.; Barfield, M.; Doddrell, D. M. *J. Chem. Phys.* **1977**, *67*, 3785−3794.
(19) Hansen, D. F.; Led, J. J. *J. Magn. Reson.* **2001**, *151*, 339−346.
(20) Ma, L.; Led, J. J. *J. Am. Chem. Soc.* **2000**, *122*, 7823−7824.

Two different types of integrals arise in eq 4 for the operator F_2^ν, depending on whether the atomic orbitals are on the same atom ($i = j$) or on different atoms ($i \neq j$). To reduce the time required for calculating Δ^2, all integrals involving overlap spin populations ($i \neq j$) are neglected. This approximation is justified by the good agreement between calculated and experimental results obtained in previous theoretical studies.[18,21−23] Thus, Δ^2 can be written as

$$\Delta^2 \simeq \frac{4\pi}{5N^2}\sum_{\nu=-2}^{2}\left|\sum_{i}^{I}\rho_i\int_V \mathrm{d}\mathbf{r}\ \psi_i(\mathbf{r})^* F_2^\nu(\mathbf{r}')\psi_i(\mathbf{r})\right|^2 \qquad (5)$$

According to eq 5, I integrals must be evaluated five times for each proton included in the analysis.

Materials and Methods

Sample Preparation. A sample of plastocyanin from *Anabaena variabilis* (*A.v.* PCu) prepared and purified as described previously[24] was kindly supplied by Jens Ulstrup and Hans E. M. Christensen, the Technical University of Denmark. The protein was dissolved in 10%/90% D_2O/H_2O or 99.99% D_2O at pH 7.0 (meter reading). Partially oxidized samples were prepared by mixing appropriate amounts of the reduced and oxidized forms of *A.v.* PCu. For the partly oxidized samples, the molar fraction, f_p, of oxidized *A.v.* PCu was 0.00, 0.11, 0.12, 0.25, and 0.47, respectively. For the samples with f_p equal to 0.00 and 0.11, the protein concentration was 3.2 mM, while it was 1.1 mM in the remaining, partly oxidized samples. A 1.8 mM 100% oxidized sample was used for measuring the relaxation rates of the hyperfine shifted signals of the protons that are spatially close to the copper(II) site. All samples contained 100 mM NaCl.

NMR Experiments. The inversion recovery TOCSY (IR-TOCSY) experiments[25] were carried out at 298.2 K and a ^{1}H frequency of 500 MHz using a Varian Unity Inova 500 spectrometer. The ^{1}H carrier was placed on the HDO resonance located at 4.77 ppm relative to TMS at 298.2 K.[26] To cover a wide range of relaxation rates, 11 relaxation delays were used in the IR-TOCSY experiments, that is, 0.00, 0.01, 0.02, 0.04, 0.10, 0.20, 0.50, 0.80, 1.20, 1.80, and 3.00 s, respectively. Each of the 11 time domain signals consisted of 512 t_1 slices, each with 4096 data points. The sweep width was 10 kHz and the mixing time in the isotropic mixing period was 50 ms.

The SERF (signal-eliminating relaxation filter) experiments,[19] which allow the observation of only the fast-relaxing nuclei, were recorded at 298.2 K and a ^{1}H frequency of 800 MHz and 500 MHz using Varian Unity Inova 800 and 500 spectrometers. The ^{1}H carrier was placed on the HDO resonance. The sweep width used in the SERF experiments was 160 kHz, and the specific SERF parameters[19] were $R_1^o = 50\ s^{-1}$, $R_1^s = 2\ s^{-1}$, $t_a = 90$ ms, and $c = 1$. In the SERF experiments, 16 relaxation delays were used, that is, 0.50, 0.71, 1.00, 1.40, 2.00, 2.80 4.00, 5.70, 8.00, 11.30, 16.00, 22.60, 32.00, 45.30, 64.00, and 90.50 ms, respectively.

Determination of the Paramagnetic Relaxation Enhancements. The R_{1p} rates of a series of protons close to the copper site were used to elucidate the delocalization of the electron spin density in oxidized *A.v.* PCu. To minimize possible errors caused by uncertainties in the solution structure of *A.v.* PCu,[16] only protons less than three residues from the copper site were included in the analysis. The R_{1p} rates of four hyperfine-shifted, fast-relaxing protons located in the immediate vicinity of the metal ion were obtained from a 100% oxidized sample using the SERF experiment.[19] Furthermore, the R_{1p} rates of five backbone protons of *A.v.* PCu were determined from partially oxidized protein samples using the IR-TOCSY experiment or the one-dimensional ^{1}H nonselective inversion recovery experiment.

The intensities of the signals used in the determination of the R_1 rates were obtained by a least-squares fitting procedure.[27] Furthermore, all intensities of a given signal in a series of partially relaxed spectra were determined simultaneously, thus exploiting the fact that the frequency, the line width, and the phase of the signal remain unchanged through the series of spectra. This procedure reduces the total number of parameters and, therefore, increases the precision of the obtained intensities. Subsequently, the relaxation rates of the protons were obtained by fitting a three-parameter single-exponential recovery to the signal intensities. Figure 2 illustrates the precision by which the relaxation rate of fast-relaxing nuclei can be determined using the SERF experiment. Both the hyperfine-shifted signals observed in the SERF spectra and the signals of the IR-TOCSY spectra were assigned previously.[16,28,29]

In the partially oxidized samples of *A.v.* PCu, exchange-averaged signals of the paramagnetic (oxidized, Cu(II)) and diamagnetic (reduced, Cu(I)) species are observed because of the electron self-exchange (ESE). If the ESE process is sufficiently fast, as in the case of *A.v.* PCu, the longitudinal relaxation of the protons is, to a good approximation, single exponential,[20,30] and the relaxation rates of the observed exchange-averaged signals are given by[30]

$$R_1 = \frac{2R_{1d} + R_{1p} + k_{ese}c}{2} - \sqrt{\left(\frac{R_{1p} + k_{ese}c}{2}\right)^2 - k_{ese}cf_pR_{1p}} \qquad (6)$$

Here, R_{1d} is the relaxation rate of the nuclei in the diamagnetic species, k_{ese} is the second-order rate constant for the ESE process, and c is the total concentration of the protein. The molar fraction, f_p, of oxidized *A.v.* PCu was estimated as described previously,[16,30] and was determined with an absolute uncertainty of 0.002−0.02. The R_{1p} and R_{1d} rates were obtained from a series of partly oxidized samples by a least-squares fit of eq 6 to a set of relaxation rates obtained for the different samples in the IR-TOCSY experiments, using the value of k_{ese} obtained previously for *A.v.* PCu.[30] Minor intermolecular contributions to the R_{1p} rates caused by interactions with other *A.v.* PCu molecules were taken into account, as described previously.[31]

The R_{1p} rates of the nine nuclei, H39 H^{β_1}, N40 H^α, F87 H^α, C89 H^{NH}, C89 H^α, E90 H^{NH}, A95 H^α, M97 H^{γ_2}, and M97 H^{NH}, are shown in Table 1. The relaxation rates of N40 H^α and M97 H^{γ_2} were measured at two different magnetic field strengths, i.e., 11.74 and 18.79 T.

Results and Discussion

Point Dipole Approximation. Qualitatively, Figure 3A reveals that the R_{1p} rates depend on the electron delocalization. If the point dipole approximation had applied, then $\Delta_{observed}^{-1/3} = r_{Cu-^1H}$, where r_{Cu-^1H} is the geometric distance between the nucleus and the copper ion in the NMR solution structure of *A.v.* PCu[16] (PDB: IFA4). However, as shown in Figure 3A, deviations from this equality are observed, which are substantially larger than the experimental uncertainties. Immediately, this suggests a breakdown of the point dipole approximation and a delocalization of the electron spin density. Furthermore, the deviations depend on the spatial position of the nuclei

(21) Barfield, M. *J. Chem. Phys.* **1970**, *53*, 3836−3843.
(22) Barfield, M. *J. Chem. Phys.* **1971**, *55*, 4682−4683.
(23) Beveridge, D.; McIver, J. W., Jr. *J. Chem. Phys.* **1971**, *54*, 4681−4690.
(24) Badsberg, U.; Jørgensen, A.-M. M.; Gesmar, H.; Led, J. J.; Hammerstad, J. M.; Jespersen, L.-L.; Ulstrup, J. *Biochemistry* **1996**, *35*, 7021−7031.
(25) Huber, J. G.; Moulis, J.-M.; Gaillard, J. *Biochemistry* **1996**, *35*, 12705−12711.
(26) Wishart, D. S.; Sykes, B. D. *Methods Enzymol.* **1994**, *239*, 363−392.
(27) Kristensen, S. M.; Sørensen, M. D.; Gesmar, H.; Led, J. J. *J. Magn. Reson. Ser. B* **1996**, *112*, 193−196.
(28) Bertini, I.; Ciurli, S.; Dikiy, A.; Gasanov, R.; Luchinat, C.; Martini, G.; Safarov, N. *J. Am. Chem. Soc.* **1999**, *121*, 2037−2046.
(29) Sato, K.; Kohzuma, T.; Dennison, C. *J. Am. Chem. Soc.* **2003**, *125*, 2101−2112.
(30) Jensen, M. R.; Hansen, D. F.; Led, J. J. *J. Am. Chem. Soc.* **2002**, *124*, 4093−4096.
(31) Hansen, D. F.; Hass, M. A. S.; Christensen, H. M.; Ulstrup, J.; Led, J. J. *J. Am. Chem. Soc.* **2003**, *125*, 6858−6859.

Table 1. Paramagnetic Relaxation Enhancements[a]

	R_{1p}(ms^{-1})	
nucleus	11.74 T	18.79 T
H39 H^{β_1}		0.622 ± 0.010[b]
N40 H^{α}	0.1827 ± 0.0005[b]	0.1152 ± 0.0007[b]
F87 H^{α}	0.009 ± 0.003[c]	
C89 H^{α}		1.53 ± 0.06[b]
C89 H^{NH}	0.36 ± 0.12[d]	
E90 H^{NH}	0.7 ± 0.2[d]	
A95 H^{α}	0.012 ± 0.002[c]	
M97 $H^{\gamma}{}_2$	0.531 ± 0.013[b]	0.304 ± 0.003[b]
M97 H^{NH}	0.084 ± 0.010[d]	

[a] Longitudinal paramagnetic relaxation enhancements at two different magnetic field strengths, used in the elucidation of the electron spin delocalization. All protons are close to the copper site in *A.v.* PCu (≤11 Å). [b] Measured with the signal-eliminating relaxation filter (SERF) experiment[19] using a 100% oxidized sample of *A.v.* PCu. [c] Measured with the IR-TOCSY experiment using partly oxidized samples of *A.v.* PCu, as described in the text. [d] Measured with one-dimensional ^{1}H nonselective inversion recovery experiments using partly oxidized samples of *A.v.* PCu, as described previously.[30]

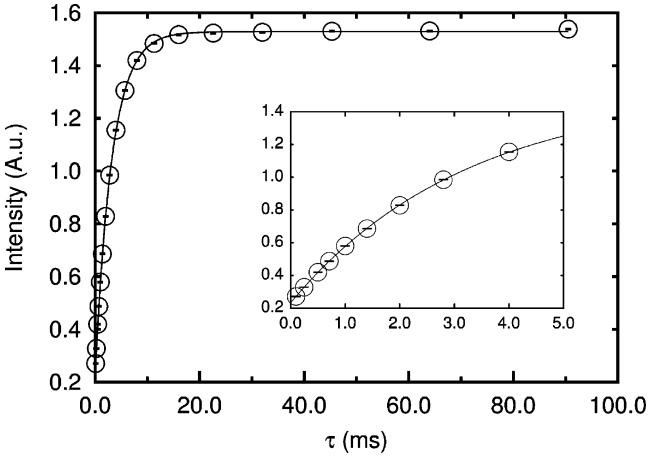

Figure 2. Single-exponential recovery of the longitudinal magnetization of M97 H^{γ_2} of *A.v.* PCu observed in the SERF experiment. The figure illustrates the quality of the experimental data and the relaxation rates obtainable in a SERF experiment. The full-drawn line corresponds to a three-parameter single-exponential fit to the experimental intensities. The insert is an expansion of the fit of the first nine intensities. The relaxation rate obtained from the least-squares fit is $R_1 = 0.305 \pm 0.002$ ms^{-1}, corresponding to $R_{1p} = R_1 - R_{1d} = 0.304 \pm 0.003$ ms^{-1} (see Table 1).

relative to the copper site, i.e., the deviations carry information about the spatial distribution of the unpaired electron spin. Therefore, the geometric factor Δ^2 in eqs 1 and 2 and, thus, the relaxation rates depend on the wave function of the unpaired electron describing the delocalization. Conversely, the delocalization can be obtained from the relaxation rates if Δ^2 is expressed as a function of the wave function.

Electron Delocalization in Plastocyanin. Plastocyanins have a type 1 blue copper site consisting of four ligands bound to the copper ion in a distorted tetrahedral geometry, as shown in Figure 1. The copper ion is covalently coordinated to the S^{γ} atom of a cysteine and to the N^{δ} atoms of two histidines. The coordination to the fourth ligand, the S^{δ} atom of a methionine, is relatively weak and the electron spin density centered at this atom is, therefore, very small and can be neglected.[1,10,12] The SOMO of the ground state is primarily described as a copper−sulfur π-antibonding orbital.[1] Furthermore, a small fraction of the electron spin density is located on the two histidines N^{δ} atoms, where the interaction with the copper is of σ-antibonding

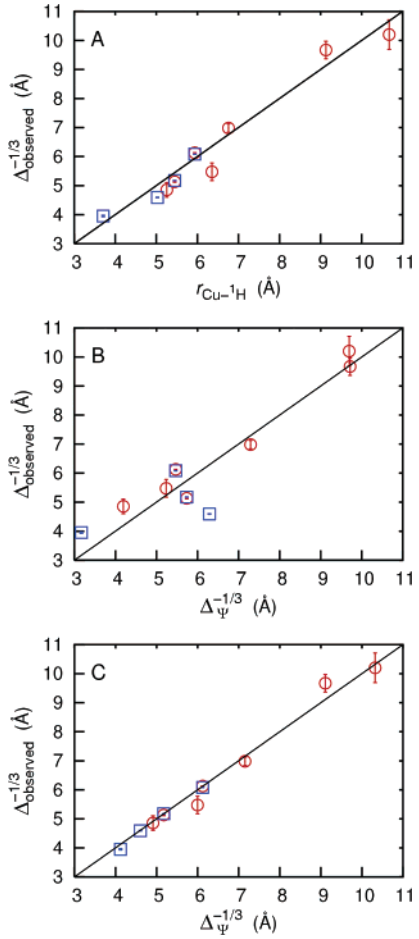

Figure 3. (A) Comparison of the geometric distances, r_{Cu-^1H}, measured in the NMR solution structure of *A.v.* PCu,[16] and the observed effective distances, $\Delta^{-1/3}_{observed}$, obtained from the paramagnetic relaxation enhancements. (B) Comparison of the calculated effective distances $\Delta^{-1/3}_{\Psi}$ and the observed effective distances, $\Delta^{-1/3}_{observed}$. The $\Delta^{-1/3}_{\Psi}$ distances were obtained from eq 5 using the spin densities found previously[1,10,12] and exemplified by the densities $\rho_{Cu} = 31.8\%$, $\rho_S = 59.1$ %, $\rho_{N_1} = 1.7\%$, and $\rho_{N_2} = 2.1\%$.[12] (C) Comparison of the calculated effective distances $\Delta^{-1/3}_{\Psi}$ and the observed effective distances, $\Delta^{-1/3}_{observed}$. The $\Delta^{-1/3}_{\Psi}$ distances were obtained from eq 5 using the spin densities in Table 2. The full-drawn lines correspond to the ideal cases, where (A) $r_{Cu-^1H} = \Delta^{-1/3}_{observed}$ and (B and C) $\Delta^{-1/3}_{\Psi} = \Delta^{-1/3}_{observed}$. The relaxation rates were obtained at two different magnetic field strengths, 11.74 T (red circles) and 18.79 T (blue squares).

character.[1,10,12] Thus, the unpaired electron spin density is primarily centered on the copper atom, the cysteine S^{γ} atom, and the two histidine N^{δ} atoms. Consequently, the total wave function of the unpaired electron can be described as a linear combination of four atomic orbitals:

$$\Psi = N^{-1/2}\left\{\sqrt{\rho_{Cu}}\psi_{Cu} + \sqrt{\rho_S}\psi_S + \sqrt{\rho_{N_{39}}}\psi_{N_{39}} + \sqrt{\rho_{N_{92}}}\psi_{N_{92}}\right\} \quad (7)$$

that is, one orbital centered on the copper atom, and three orbitals are centered on the covalently bound ligand atoms, the unpaired electron spin densities being ρ_{Cu}, ρ_S, $\rho_{N_{39}}$, and $\rho_{N_{92}}$, respectively. In eq 7, N is a normalization coefficient. Furthermore, the spin densities are assumed to be positive and real. Previously, it was concluded from EPR experiments and optical absorption spectra[1,2] that the four orbitals are a $3d_{x^2-y^2}$-type

orbital on the copper atom, a $1/\sqrt{2}(3p_x - 3p_y)$-type orbital on the S^γ atom of the cysteine, and $2p_y$- and $-2p_x$-type orbitals on the N^δ atoms of the two histidines. In the analysis here, all four orbitals were represented by real hydrogen-like atomic orbitals, where the effective nuclear charges were found by the Slater rule, i.e., Cu : 8.20*e*, S^γ : 5.45*e*, N^δ : 3.90*e*, *e* being the elementary charge. The geometric factor, Δ^2, can now be written as a function of the spin densities ρ_{Cu}, ρ_S, $\rho_{N_{39}}$, and $\rho_{N_{92}}$ according to eq 5, and the spin densities can be determined using eq 1, if a sufficient number of accurate R_{1p} rates can be measured and if the three-dimensional structure of the protein is known. Both of these requirements are fulfilled here.

Conversely, R_{1p} rates can be calculated from the spin densities found previously by quantum chemical calculations,[1,10,12] thereby providing an assessment of these calculations. Thus, using eq 5, effective distances, $\Delta_\Psi^{-1/3}$, were calculated from theoretical spin densities and, using eq 1, compared with the corresponding distances obtained from the experimental paramagnetic relaxation enhancements (Table 1). This was done for the nine protons close to the copper(II) site, for which precise R_{1p} rates were measured. As shown in Figure 3B, the two sets of distances do not agree, that is, the large delocalization of the electron spin found previously by the quantum chemical calculations is at variance with the experimentally measured relaxation rates. Clearly, this disagreement calls for the direct determination of the electron delocalization from the experimental paramagnetic relaxation rates, described here.

Consequently, integrals of the type given in eq 5 were evaluated analytically for each of the nine protons close to the copper(II) site (see Table 1). The F_2^ν operators are the spatial part of the dipole operators, and ψ_i in eq 5 are the individual atomic orbitals onto which the unpaired electron spin is delocalized. The F_2^ν operators were centered on the nuclei, while the $\mathbf{r}_{Cu-^1H}$ vectors used in the evaluation of the integrals were obtained from the NMR solution structure of *A.v.* PCu.[16] Subsequently, Δ^2 (eq 5) was expressed as a function of the four unknown spin densities, ρ_{Cu}, ρ_S, $\rho_{N_{39}}$, and $\rho_{N_{92}}$, for each nuclei included in the analysis, using eq 7. Finally, an over-determined set of equations in the four unknown spin densities was formed using the integrals (eq 5) in conjunction with eq 1 and the measured paramagnetic relaxation enhancements. In principle, this set of equations allows an estimation of all four spin densities by a least-squares analysis. Yet, the information provided by the R_{1p} rates obtained here is not sufficient for this estimation. However, the distorted tetrahedron of the copper site has pseudo-C_s symmetry (see Figure 1) with the mirror plane bisecting the bonding vectors from the copper to the two N^δ atoms. Therefore, the N^δ atoms of the two histidines have identical electron spin densities. This conclusion was confirmed by previous ENDOR measurements,[13] which showed that the hyperfine coupling constants of the two ligand N^δ atoms are identical. By utilizing this symmetry, a least-squares fit to the experimental R_{1p} rates, using the combined set of equations described above, resulted in the electron spin densities on the four involved nuclei given in Table 2.

When the Δ^2 values are calculated from these spin densities using eqs 1, 5, and 7, the substantial deviations from the experimental data observed in Figures 3A and 3B vanish, as shown in Figure 3C. Thus, the paramagnetic relaxation enhancements clearly reveal not only that the unpaired electron spin is delocalized, although not to the same degree as predicted by the quantum chemical calculations; they also allow a quantitative mapping of the electron spin delocalization. Moreover, the contour plot of the total electron spin density, $|\Psi|^2$, in Figure 4 shows that the C89 S^γ 3p orbital is considerably more delocalized than the Cu $3d_{x^2-y^2}$ orbital, despite the much smaller spin density in this orbital. This inflation of the 3p orbital of C89 S^γ is caused by the smaller effective charge of the S atom as compared to the Cu atom. Therefore, the delocalized spin density at the C89 S^γ ligand reaches far out into the protein. This, in turn, may reflect the function of the protein, i.e., its capability of long-range, rapid, and directional electron transfer.

Table 2. Spin Densities of the Active Site in *A.v.* PCu[a]

ρ_{Cu} (%)	ρ_S (%)[b]	$\rho_{N_{39}}$(%)[c]	$\rho_{N_{92}}$ (%)[d]
84.3 ± 2.3	10.9 ± 0.6	2.5 ± 1.5	2.5 ± 1.5

[a] Obtained from a least-squares fit of eq 5 to the measured paramagnetic relaxation enhancements in Table 1 of nine protons close to the copper(II) site in *A.v.* PCu. [b] C89 S^γ. [c] H39 N^δ. [d] H92 N^δ.

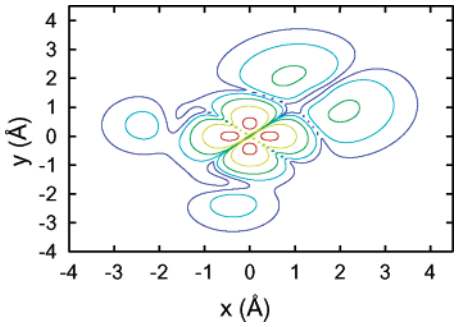

Figure 4. Contour plot of the electron spin density $|\Psi|^2$ (eq 7) using the spin densities in Table 2. Red lines correspond to $|\Psi|^2 = 1.0$ Å^{-3}; yellow lines correspond to $|\Psi|^2 = 0.10$ Å^{-3}; green lines correspond to $|\Psi|^2 = 10^{-2}$ Å^{-3}; light blue lines correspond to $|\Psi|^2 = 10^{-3}$ Å^{-3}; and dark blue lines correspond to $|\Psi|^2 = 10^{-4}$ Å^{-3}. The plane of the paper is the *x*,*y*-plane of the coordinate system, i.e., $z = 0$. The Cartesian coordinates of the atoms are: Cu = (0, 0, 0), C89; S^γ = (1.416, 1.416, − 0.684), H39; N^δ = (−0.376, −1.874, −0.693), H92; N^δ = (−1.865, 0.385, −0.724). All coordinates are in Ångströms.

Conclusion

In conclusion, it is experimentally verified by longitudinal paramagnetic NMR relaxation that the unpaired electron spin density of oxidized *A.v.* PCu is delocalized onto the ligands. Furthermore, a quantitative mapping of the electronic structure of the blue copper site is obtained from the paramagnetic NMR relaxation rates. The approach used here is applicable as long as a sufficient number of accurate R_{1p} rates can be measured, the three-dimensional structure of the protein is known, and the ligand orbitals to which the electron spin is delocalized are identified. The electron spin delocalization obtained here is of particular interest since it is determined directly for a native plastocyanin in solution and not for a model complex. Therefore, it provides a direct basis for a better understanding of the long-range and rapid electron-transfer reactivity that characterizes blue copper proteins.

Acknowledgment. We thank Malene R. Jensen, Sten Rettrup, and Michael Barfield for helpful discussions, Hans E. M.

Christensen and Jens Ulstrup for providing the plastocyanin samples, and Lise-Lotte Jespersen, Else Philipp, Jens Duus, Charlotte Gotfredsen, and Bent O. Petersen for technical assistance. The 800 MHz spectra were acquired at The Danish Instrument Center for NMR Spectroscopy of Biological Macromolecules. D.F.H. thanks Novo Nordisk A/S and Novozymes A/S for a scholarship. This work was financially supported by the Danish Natural Science Research Council J. Nos. 9400351, 51-00211, and 21-01-0545, and the Danish Technical Research Council J. No. 26-03-0055.

JA0379464